Constrained Corticotropin-Releasing Factor (CRF) Agonists and Antagonists with *i*−(*i*+3) Glu-Xaa-DXbb-Lys Bridges†

Steven C. Koerber, Jozsef Gulyas, Sabine L. Lahrichi, Anne Corrigan, A. Grey Craig, Catherine Rivier, Wylie Vale, and Jean Rivier*

The Clayton Foundation Laboratories for Peptide Biology, The Salk Institute for Biological Studies, 10010 North Torrey Pines Road, La Jolla, California 92037

Received June 8, 1998

We hypothesized that covalent constraints such as side-chain to side-chain lactam rings would stabilize an α-helical conformation shown to be important for the recognition and binding of the human corticotropin-releasing factor (hCRF) C-terminal 33 residues to CRF receptors. These studies led to the discovery of cyclo(20−23)[DPhe^{12},Glu^{20},Lys^{23},Nle^{21,38}]hCRF$_{(12-41)}$ and of astressin {cyclo(30−33)[DPhe^{12},Nle^{21,38},Glu^{30},Lys^{33}]hCRF$_{(12-41)}$}, two potent CRF antagonists, and of cyclo(30−33)-[Ac-Leu^{8},DPhe^{12},Nle^{21},Glu^{30},Lys^{33},Nle^{38}]hCRF$_{(8-41)}$, the shortest sequence equipotent to CRF reported to date (Rivier et al. *J. Med. Chem.* **1998**, *41*, 2614−2620 and references therein). To test the hypothesis that the Glu^{20}−Lys^{23} and Glu^{30}−Lys^{33} lactam rings were favoring an α-helical conformation rather than a turn, we introduced a D-amino acid at positions 22, 31, and 32 in the respective rings. Whereas the introduction of a D-residue at position 31 was only marginally deleterious to potency (ca. 2-fold decrease in potency), introduction of a D-residue at position 22 and/or 32 was favorable (up to 2-fold increase in potency) in most of the cyclic hCRF, α-helical CRF, urotensin, and urocortin agonists and antagonists that were tested and was also favorable in linear agonists but not in linear antagonists; this suggested a unique and stabilizing role for the lactam ring. Introduction of a [DHis^{32}] (**6**) or acetylation of the N-terminus (**7**) of astressin had a minor deleterious or a favorable influence, respectively, on duration of action. In the absence of structural data on these analogues, we conducted molecular modeling on an Ac-Ala$_{13}$-NH$_2$ scaffold in order to quantify the structural influence of specific L- and DAla^{6} and L- and DAla^{7} substitutions in [Glu^{5},-Lys^{8}]Ac-Ala$_{13}$-NH$_2$ in a standard α-helical configuration. Models of the general form [Glu^{5},LAla^{6} or DAla^{6},LAla^{7} or DAla^{7},Lys^{8}]Ac-Ala$_{13}$-NH$_2$ were subjected to high-temperature molecular dynamics followed by annealing dynamics and minimization in a conformational search. A gentle restraint was applied to the 0−4, 1−5, and 8−12 O−H hydrogen bond donor−acceptor pairs to maintain α-helical features at the N- and C-termini. From these studies we derived a model in which the helical N- and C-termini of hCRF form a helix−turn−helix motif around a turn centered at residue 31. Such a turn brings Gln^{26} in close enough proximity to Lys^{36} to suggest introduction of a bridge between them. We synthesized dicyclo(26−36,30−33)[DPhe^{12},Nle^{21},Cys^{26},Glu^{30},Lys^{33},Cys^{36},Nle^{38}]-Ac-hCRF$_{(9-41)}$ which showed significant α-helical content using circular dichroism (CD) and had low, but measurable potency {0.3% that of **6** or ca. 25% that of [DPhe^{12},Nle^{21,38}]hCRF$_{(12-41)}$}. Since the 26−36 disulfide bridge is incompatible with a continuous α-helix, the postulate of a turn starting at residue 31 will need to be further documented.

Introduction

We have shown that corticotropin-releasing factor (CRF), a peptide first isolated and characterized from sheep hypothalami,[2] is a key modulator of the stress response and plays a major role in the maintenance or restoration of homeostasis by regulating the activity of the hypothalamic−pituitary−adrenal (HPA) axis.[3] The actions of CRF are mediated through binding to two classes of seven-transmembrane-helix G-protein-coupled CRF receptors.[4−10] ACTH release from the pituitary results from activation of CRFR1 receptors. CRF is considered to stimulate many of the functions that help the organism survive (such as locomotor activity and catecholamine release) while inhibiting those that might interfere with an effective stress response (such as feeding and sexual behavior).[11] For example, through the release of glucocorticoids, CRF alters immune parameters[12] and participates in the regulation of carbohydrate metabolism by enhancing the availability of glucose (reviewed in Dallman et al.[13]). CRF also regulates behavior and vegetative functions including cardiovascular responses mediated by CRFR2. Our interest in understanding the structure−activity rela-

† Abbreviations: IUPAC rules are used for nomenclature of peptides including one-letter codes for amino acids. Also: Ac, acetyl; ACTH, adrenocorticotropin hormone; Acn, acetonitrile; astressin, cyclo(30−33)[DPhe^{12}, Nle^{21,38},Glu^{30}, Lys^{33}]hCRF$_{(12-41)}$; Boc, *tert*-butyloxycarbonyl; BOP, benzotriazolyloxy-tris(dimethylamino)phosphonium hexafluorophosphate; BSA, bovine serum albumin; CD, circular dichroism; CRF, corticotropin-releasing factor (o, ovine; h, human); CRFR, CRF receptor; CVFF, consistent valence force field; CZE, capillary zone electrophoresis; DCM, dichloromethane; DIC, diisopropylcarbodiimide; DMF, dimethylformamide; FBS, fetal bovine serum; Fmoc, 9-fluorenylmethoxycarbonyl; HBTU, *O*-(benzotriazol-1-yl)-*N*,*N*,*N*′,*N*′-tetramethyluronium hexafluorophosphate; HF, hydrogen fluoride; IA, intrinsic activity; MBHAR, 4-methylbenzhydrylamine resin; 2Nal, 2-naphthylalanine; NMP, *N*-methylpyrrolidinone; OFm, *O*-fluorenylmethyl; PTH, parathyroid hormone; rms, root-mean-square; SAR, structure−activity relationships; Sau, sauvagine; TBTU, *O*-(benzotriazol-1-yl)-*N*,*N*,*N*′,*N*′-tetramethyluronium tetrafluoroborate; TEAP 2.25, 4.5, and 6.5, triethylammonium phosphate, pH 2.25, 4.5, and 6.5; TFA, trifluoroacetic acid; TFE, trifluoroethanol; Ucn, urocortin; cUtn, carp urotensin; sUtn, sucker fish urotensin; Xaa and Xbb, three-letter codes for any amino acid.

* Author for correspondence.

10.1021/jm980350k CCC: $15.00
Published on Web 11/12/1998

tionships (SAR) of CRF stems from the belief that conditions characterized by too little or too much CRF might be alleviated by the administration of long-acting CRF agonists or antagonists, respectively.

We have shown that deletion of the first 8−14 residues of CRF leads to antagonists with varying potencies. Whereas the first antagonist [α-helical $CRF_{(9-41)}$] was 33 residues long, the next generation of antagonists, [DPhe^{12},Nle^{21,38}]h$CRF_{(12-41)}$ and [DPhe^{12},-C$^{\alpha}$MeLeu^{37},Nle^{21,38}]h$CRF_{(12-41)}$, were 3 residues shorter.[14] More recently, we described the effect of the introduction of lactam rings such as Glu-Xaa-Xbb-Lys or Glu-Xaa-Xbb-Xcc-Lys on the potency of CRF antagonists.[15,16] More precisely, cyclo(20−23)[DPhe^{12},Glu^{20},Lys^{23},Nle^{21,38}]-h$CRF_{(12-41)}$17 and cyclo(30−33)[DPhe^{12},Glu^{30},Lys^{33},-Nle^{21,38}]h$CRF_{(12-41)}$ (astressin)[16] were 3 and 32 times as potent as [DPhe^{12},Nle^{21,38}]h$CRF_{(12-41)}$, respectively, with extended duration of action in vivo. In the CRF agonist series (analogues that are extended at the N-terminus as compared to the antagonists) we reported that the introduction of the cyclo(30−33) Glu-Xaa-Xbb-Lys did not increase potency significantly as compared to that of the corresponding linear analogue and was only 3 times more potent than CRF itself.[16]

The present study first describes the effect of the introduction of D-amino acids within the cycles formed between residues 20 and 23 and residues 30 and 33 in CRF agonists and antagonists. These substitutions were introduced to validate the postulate that the introduction of a D-residue at positions 22, 31, and 32 would have dramatic effects on the structures of the respective cycles and of the overall molecules such as favoring one or two turn(s) around residues 20−23 and 30−33 over the hypothesis that CRF's bioactive conformation is essentially α-helical from residues 5 to 41. Whereas there is no theoretical precedent for a turn in the region of residues 20−23 of CRF, a turn has been postulated for residues 30−33 of CRF, sauvagine, and urotensin.[18] A priori, the Glu^{30}-Xaa-Xbb-Lys^{33} bridge could be stabilizing a turn rather than a helix, although there is some evidence (NMR[19] and CD[15]) to the contrary. This hypothesis led to a theoretical investigation, as well as the synthesis, of a dicyclic CRF antagonist and a significant number of analogues of members of the CRF family with side-chain to side-chain bridges and the additional constraints brought about by the introduction of D-residues within the ring structures. We had already investigated the effect of inversion of chirality at the bridgeheads in the antagonist series[15] and concluded that LGlu and LLys, in that order, were most favored at positions 20, 23 and 30, 33. Linear antagonists with D-residues at positions 21, 22, 31, and 32 were not synthesized because these substitutions are not well-tolerated in oCRF[20] or in the linear antagonists corresponding to the cyclic analogues having substitutions at positions 20, 23, 30, and 33 (the bridgeheads).[16,17] We also describe the effect of the accumulation of two favorable cycles (cyclo(20−23) and cyclo(30−33)) in one CRF analogue to check the possibility that two favorable ring structures would have an additive/multiplicative effect on potency. Structures of some of the analogues described here were investigated by CD. Finally, we hypothesized that the cumulative effect of acetylation of the N-terminus and introduction of a D-amino acid at position 32 would increase stability against enzymatic degradation resulting in increased duration of action. These analogues were tested in the adrenalectomized rat for their effect on inhibition of release of adrenocorticotropin (ACTH) and the duration of such effect after a single iv injection.

Results and Discussion

All analogues shown in Table 1 were synthesized on a methylbenzhydrylamine resin (MBHAR) using the Boc strategy with orthogonal protection of the side chains of the lysine (Fmoc) and glutamic acid (OFm) residues to be cyclized.[1,15,17,21] Main-chain assembly was mediated in most cases by diisopropylcarbodiimide (DIC). The best results were obtained when the peptide chain was assembled in its entirety prior to cleavage of the Fmoc and OFm protecting groups and when the lactam formation was mediated by TBTU or BOP.[15] Oxidation of cysteine residues in **8**, which occurred very slowly when the solution was exposed to air, was mediated by the slow addition of H_2O_2 to the acidic (0.1% TFA/48% Acn) solution containing the HPLC-purified, reduced cyclo(30−33) peptide. The peptides were cleaved and deprotected in HF at 0 °C in the presence of a scavenger and purified with HPLC using linear gradients of Acn in three aqueous buffers (except for **8**, see Experimental Section) (TEAP 2.25, TEAP 4.5, or TEAP 6.5 and 0.1% TFA).[1,15,22,23] The critical step in obtaining highly purified CRF analogues was the use of a TEAP buffer at a pH higher than 4.5. Under those conditions, impurities in amounts close to 30% that were difficult to detect in other buffer systems were eliminated. Although very difficult to demonstrate, we have found that those impurities (probably no single species was present in an amount greater than 1%) could interfere with sensitive in vitro and in vivo assays. Peptides were characterized as shown in Table 1. Most analogues were determined to be greater than 95% pure using RP-HPLC and CZE criteria. The measured masses obtained using liquid secondary ion mass spectrometry were in agreement with those calculated for the protonated molecule ions.

To refine models of CRF and identify structural components which can be constrained by peptidomimetic functionalities, several strategies were employed. We have identified, using molecular dynamics and energy minimization, α-helical conformations and turn-encompassing structures energetically available to the analogues. Comparison of structures by calculation of the rms deviations over the backbone atoms of optimally superposed pairs allowed the identification of commonly available conformations.

The CD spectra of a number of analogues were recorded in an attempt to correlate activity with structure. Earlier studies[14,15] had shown that significant β-sheet and random coil-type structures characterized most of the compounds under aqueous conditions as judged by spectral deconvolution using the method of Yang et al.[24] On the other hand, in 50% TFE, significant α-helical structure is induced in all compounds with concomitant reduction in β-sheet and turn structures. No obvious correlation could be found between biological activity and secondary structural features observed in CD. In the current work, the CD spectra

Table 1. CRF Antagonists and Agonists with *i*, (*i*+3) Bridge and D-residue at *i*, (*i*+2)

	5	10	15	20	25	30	35	40
Human CRF	S E E P P I S L D L T F H L L R E V L E M A R A E Q L A Q Q A H S N R K L M E I I-NH_2							
α-helical CRF	S Q E P P I S L D L T F H L L R E M L E M A K A E Q E A E Q A A L N R L L L E E A-NH_2							
carp Urotensin	N D D P P I S I D L T F H L L R N M I E M A R N E N Q R E Q A G L N R K Y L D E V-NH_2							
sucker Urotensin	N D D P P I S I D L T F H L L R N M I E M A R I E N E R E Q A G L N R K Y L D E V-NH_2							
human Urocortin	D N P S L S I D L T F H L L R T L L E L A R T Q S Q R E R A E Q N R I I F D S V-NH_2							
Sauvagine	pE G P P I S I D L S L E L L R K M I E I E K Q E K E K Q Q A A N N R L L L D T I-NH_2							

no.	compound	HPLC[a]	CZE[b]	MS (mono)[c] calcd	MS (mono)[c] found	rel. potencies[d] in vitro	IA[e]	ref
	CRF Antagonists							
1	cyclo(20−23)[DPhe^{12},Glu^{20},Nle,^{21,38}Lys^{23}]hCRF$_{(12-41)}$	>97	>97	3491.99	3491.7	2.9 (1.3−6.7)‡	11	17
2	[DPhe^{12},Glu^{20},Nle,^{21,38}Lys^{23}]hCRF$_{(12-41)}$	>97	>97	3510.01	3510.0	0.31 (0.14−0.65)‡	42	17
3	cyclo(30−33)[DPhe^{12},Nle,^{21,38}Glu^{30},Lys^{33}]hCRF$_{(12-41)}$ (astressin)	90	94	3562.13	3562.2	32‡ *f*	0−5	16
4	[DPhe^{12},Nle,^{21,38}Glu^{30},Lys^{33}]hCRF$_{(12-41)}$	96	94	3580.06	3580.1	0.10 (0.06−0.16)‡ *f* 0.04 (0.01−0.12)‡	0 5	17
5	cyclo(30−33)[DPhe^{12},Nle,^{21,38}Glu^{30},DAla^{31},Lys^{33}]hCRF$_{(12-41)}$	94	97	3562.05	3561.7	17 (6.6−42)‡		
6	cyclo(30−33)[DPhe^{12},Nle,^{21,38}Glu^{30},DHis^{32},Lys^{33}]hCRF$_{(12-41)}$	97	>97	3562.05	3562.4	56‡ 1.00‡‡	19	
7	cyclo(30−33)[Ac-DPhe^{12},Nle,^{21,38}Glu^{30},DHis^{32},Lys^{33}]hCRF$_{(12-41)}$	94	90	3604.06	3604.1	1.2 (0.41−3.3)‡‡	10	
8	dicyclo(26−36,30−33)[Ac-Asp^{9},DPhe^{12},Nle,^{21,38}Cys^{26},Glu^{30},Lys^{33},-Cys^{36}]hCRF$_{(9-41)}$	>97	>97	3881.06	3881.0	0.26 (0.14−0.49)‡ 0.003 (0.001−0.009)‡‡	0	
9	cyclo(30−33)[DPhe^{12},Nle,^{21,38}Glu^{30},DAla^{31},DHis^{32},Lys^{33}]hCRF$_{(12-41)}$	>97	>97	3562.05	3562.0	0.07 (0.03−0.14)‡‡	13	
10	dicyclo(20−23,30−33)[DPhe^{12},Glu^{20},Nle,^{21,38}Lys^{23},Glu^{30},Lys^{33}]-hCRF$_{(12-41)}$	96	>97	3516.03	3516.0	8.3 (3.7−18)‡	49	17
11	dicyclo(20−23,30−33)[DPhe^{12},Glu^{20},Nle,^{21,38}DAla^{22},Lys^{23},Glu^{30},-DHis^{32},Lys^{33}]hCRF$_{(12-41)}$	97	97	3516.03	3516.0	8.6 (4.6−16)‡	6	
12	cyclo(30−33)[DPhe^{12},Nle,^{18,21}Glu^{30},DAla^{32},Lys^{33}]cUtn$_{(12-41)}$	>97	>97	3662.96	3663.1	0.83 (0.33−2.0)‡	2	
13	cyclo(29−32)[DLeu^{11},Nle,^{17}Glu^{29},Lys^{32}]Sau$_{(11-40)}$	>97	97	3586.11	3586.1	0.28 (0.12−0.59)‡	18	
14	cyclo(29−32)[DLeu^{11},Nle,^{17}Glu^{29},DAla^{31},Lys^{32}]Sau$_{(11-40)}$	97	>97	3586.11	3586.2	0.19 (0.069−0.46)‡	25	
15	cyclo(29−32) [DPhe^{11},Glu^{29},DGlu^{31},Lys^{32}]hUcn $_{(11-40)}$	>97	>97	3593.97	3593.8	4.7 (2.2−10.0)‡	19	
16	cyclo(29−32)[Pro^{10},DPhe^{11},Glu^{29},DGlu^{31},Lys^{32}]hUcn $_{(10-40)}$	>97	>97	3691.02	3690.9	2.7 (1.0−8.0)‡	23	
17	cyclo(29−32)[DPro^{10},DPhe^{11},Glu^{29},DGlu^{31},Lys^{32}]hUcn $_{(10-40)}$	>97	>97	3691.02	3691.0	5.0 (2.3−12)‡	25	
18	cyclo(30−33)[DPhe^{12},Nle,^{21,38}Glu^{30},DNal,^{32}Lys^{33}]hCRF$_{(12-41)}$	90	>97	3622.07	3621.7	0.23 (0.1−0.49)‡‡	50	
19	cyclo(30−33)[DPhe^{12},Nle,^{21,38}Glu^{30},DGlu^{32},Lys^{33}]hCRF$_{(12-41)}$	97	>97	3554.03	3554.2	0.12 (0.060−0.27)‡‡	24	
20	cyclo(30−33)[DPhe^{12},Nle,^{21,38}Glu^{30},DArg^{32},Lys^{33}]hCRF$_{(12-41)}$	97	>97	3581.09	3581.3	0.75 (0.33−1.7)‡‡	10	
	CRF Agonists							
21	cyclo(20−23)[Ac-Pro^{4},DPhe^{12},Glu^{20},Nle,^{21,38}Lys^{23}]hCRF$_{(4-41)}$	95	96			9.4 (4.7−20)(h)		
22	cyclo(20−23)[Ac-Pro^{4},DPhe^{12},Glu^{20},Nle,^{21,38}DAla^{22},Lys^{23}]hCRF$_{(4-41)}$	>97	95	4370.47	4370.5	4.4 (2.2−9.1)(h)		
23	[Ac-Pro^{4},DPhe^{12},Glu^{20},Nle,^{21,38}DAla^{22},Lys^{23}]hCRF$_{(4-41)}$	97	>97	4388.48	4388.5	4.8 (2.3−11)(h)		
24	cyclo(30−33)[Ac-Pro^{4},DPhe^{12},Nle,^{21,38}Glu^{30},Lys^{33}]hCRF$_{(4-41)}$	96	95	4440.52	4440.4	6.0 (3.0−13)(o)*f* 6.3 (3.2−12.9)(h) 4.3 (2.5−7.8)(h)		16
25	[Ac-Pro^{4}-DPhe^{12},Nle,^{21,38}Glu^{30},Lys^{33}]hCRF$_{(4-41)}$	96	95	4458.54	4458.6	4.5 (2.7−7.6)(h)*f* 4.0 (2.3−7.2)(h)		16
26	cyclo(30−33)[Ac-Pro^{4},DPhe^{12},Nle,^{21,38}Glu^{30},DHis^{32},Lys^{33}]hCRF$_{(4-41)}$	96	97	4440.52	4440.5	3.7 (2.1−6.2)(h)*f* 5.9 (3.3−11)(h) 7.7 (1.9−26)(h)		
27	cyclo(30−33)[Ac-Pro^{4},DPhe^{12},Nle,^{21,38}Glu^{30},DAla^{31},Lys^{33}]hCRF$_{(4-41)}$	97	N/A	4440.52	4440.5	1.5 (0.8−2.7)(o)		
28	dicyclo(20−23,30−33)[Ac-Pro^{4},DPhe^{12},Glu^{20},Nle,^{21,38}DAla^{22},Lys^{23},-Glu^{30},DHis^{32},Lys^{33}]hCRF$_{(4-41)}$	93	96	4394.51	4394.6	1.1 (0.57−2.0)(h)		
29	cyclo(30−33)[Ac-Pro^{4},DPhe^{12},Glu^{30},Lys^{33}]α-hel-CRF$_{(4-41)}$	95	94	4336.36	4336.4	7.5 (4.6−12)(h)		1
30	cyclo(30−33)[Ac-Pro^{4},DPhe^{12},Nle,^{18,21}Glu^{30},DAla^{32},Lys^{33}]α-hel-CRF$_{(4-41)}$	>97	96	4336.36	4336.6	6.8 (3.8−12)(h)		
31	[Ac-Pro^{4},DPhe^{12},Nle,^{18,21}DAla^{32}]α-hel-CRF$_{(4-41)}$	>97	>97	4338.4	4338.4	2.1 (1.0−4.3)(h)		
32	cyclo(30−33)[DPhe^{12},Nle,^{18,21}Glu^{30},Lys^{33}]sUtn	96	96	4829.53	4829.8	2.9 (1.3−6.6)(h)		1
33	cyclo(30−33)[Ac-Pro^{4},DPhe^{12},Nle,^{18,21}Glu^{30},DAla^{32},Lys^{33}]cUtn$_{(4-41)}$	>97	97	4541.44	4541.8	17 (9.5−31)(h)		
34	[Ac-Pro^{4},DPhe^{12},Nle,^{18,21}Glu^{30},DAla^{32},Lys^{33}]cUtn$_{(4-41)}$	92	95	4559.45	4559.4	2.2 (1.5−3.2)(h)		
35	cyclo(29−32)[Ac-Pro^{3},DPhe^{11},Glu^{29},Lys^{32}]hUcn$_{(3-40)}$	95	95	4462.42	4462.5	3.8 (2.5−5.8)(h)		1
36	cyclo(29−32)[Ac-Pro^{3},DPhe^{11},Glu^{29},DGlu^{31},Lys^{32}]hUcn$_{(3-40)}$	>97	96	4462.42	4562.4	6.1 (2.8−14)(h)		
37	[Ac-Pro^{3},DPhe^{11},Glu^{29},DGlu^{31},Lys^{32}]hUcn$_{(3-40)}$	>97	>97	4480.43	4480.4	0.96 (0.38−2.7)(h)		
38	cyclo(29−32)[DLeu^{11},Nle,^{17}Glu^{29},Lys^{32}]sauvagine	95	>97	4576.61	4576.7	5.7 (2.6−14)(o)		1
39	cyclo(29−32)[Ac-Pro^{3},DLeu^{11},Nle,^{17}Glu^{29},DAla^{31},Lys^{32}]Sau $_{(3-40)}$	>97	>97	4450.56	4450.5	5.4 (2.9−10)(h)		
40	[Ac-Pro^{3},DLeu^{11},Nle,^{17}Glu^{29},DAla^{31},Lys^{32}]Sau$_{(3-40)}$	>97	97	4468.58	4468.7	0.018 (0.010−0.031)(h)		

[a] Percent purity determined by HPLC using buffer system: A = TEAP (pH 2.5) and B = 60% CH_3CN/40% A with a gradient slope of 1% B/min, at flow rate of 0.2 mL/min on a Vydac C_{18} column (0.21 × 15 cm, 5-μm particle size, 300-Å pore size), detection at 214 nm. [b] Capillary zone electrophoresis (CZE) was done using a Beckman P/ACE System 2050 controlled by an IBM Personal System/2 model 50Z and using a ChromJet integrator; field strength of 15 kV at 30 °C, mobile phase 100 mM sodium phosphate (85:15 H_2O-CH_3CN), pH 2.50, on a Supelco P175 capillary (363-μm o.d. × 75-μm i.d. × 50-cm length), detection at 214 nm. CZE was carried out in the presence of 30% acetonitrile. [c] The observed *m*/*z* of the monoisotope compared with the calculated $[M + H]^+$ monoisotopic mass. [d] Antagonist potencies are relative to that of [DPhe^{12},Nle^{21,38}]hCRF$_{(12-41)}$‡ or to that of cyclo(30−33)[DPhe^{12},Nle,^{21}Glu^{30},DHis^{32},Lys^{33},Nle^{38}]hCRF$_{(12-41)}$‡‡ (**6**) in the in vitro rat pituitary cell culture assay, with 95% confidence limits in parentheses. Potency of **6** relative to that of [DPhe^{12},Nle^{21,38}]hCRF$_{(12-41)}$‡ and IA are the average from data obtained in three independent assays [80.3 (41.6−173), IA 30; 68.6 (38.2−

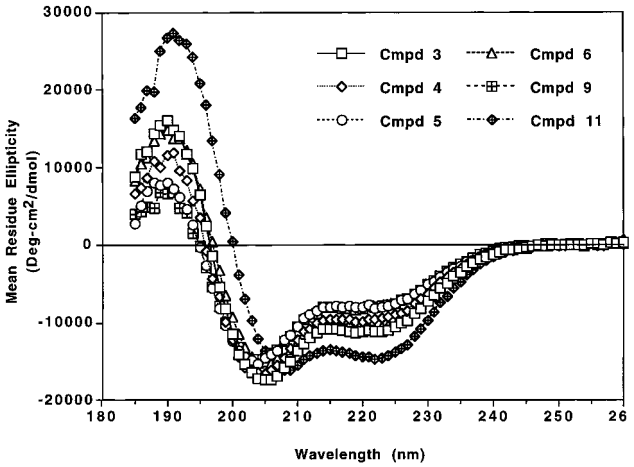

Figure 1. Circular dichroic spectra of compounds **3**−**6**, **9**, and **11** in water.

Table 2. Deconvolution of CD Spectra of CRF Analogues **3**−**6**, **9**, and **11** by the Method of Böhm et al.[25]

CD component (%)	compound					
	3	**4**	**5**	**6**	**9**	**11**
helix	28.9	21.9	16.2	27.6	16.0	45.8
antiparallel sheet	3.3	6.8	13.7	4.4	13.8	2.4
parallel sheet	6.1	4.6	3.7	6.0	3.6	8.7
β-turn	31.3	33.8	33.8	29.5	33.9	20.2
random coil	42.9	38.5	34.8	40.6	34.9	35.5
total %	112.5	105.6	102.2	108.1	102.2	112.6

of **3**−**6**, **9**, and **11** were recorded in aqueous solution. As shown in Figure 1, all of the compounds, based on astressin, have some helical content as judged by the observation of extrema at ca. 222, 208, and 195 nm. As before, no correlation was found in these compounds with helicity determined by the intensity or position of CD absorbances and biological potency. Deconvolution (Table 2) of the spectra of Figure 1 by the neural network method of Böhm et al.[25] employed the 33-compound basis set over the wavelength range of 260−185 nm. The fit was considered semiquantitative because the summed percentages of secondary structural type deviated significantly from 100% for **3**, **6**, and **11**, which may be due in large part to the small size of these CRF analogues and the relatively larger size of the basis proteins. However, clearly all of the compounds shown in Figure 1 have helical character in aqueous solution, and the helix is observed even in the absence of the 30−33 lactam (compare **3** and **4**).

CRF analogues (**21**−**40**) were tested for agonist activity in an in vitro assay measuring release of ACTH by rat anterior pituitary cells in culture.[2,26,27] Since the studies were carried out over a prolonged period of time, relative potencies with 95% confidence limits in parentheses are shown using either oCRF or hCRF as the assay standard with a potency equal to 1.0 (Table 1). Both oCRF and hCRF are essentially equipotent in this assay.[28] CRF antagonists (**1**−**20**) were tested in the same pituitary cell culture assay which measured their

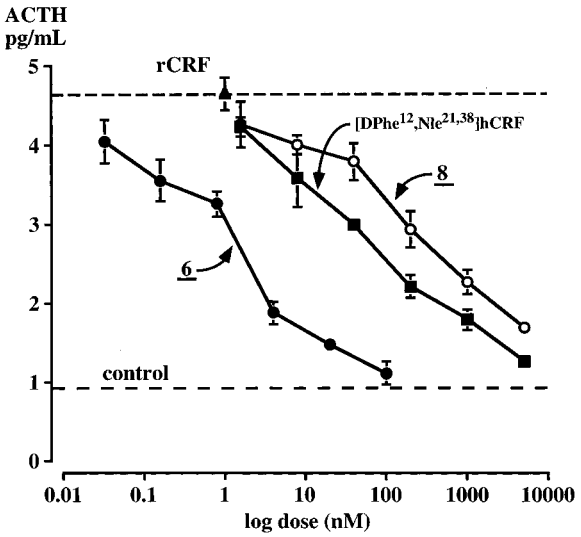

Figure 2. Interaction between 1 nM CRF and increasing doses of CRF antagonists on ACTH secretion by rat anterior pituitary cells in monolayer culture.

ability to inhibit ACTH release stimulated by 1 nM CRF. Several agonists and antagonists (**4**, **6**, **24**−**26**) were tested more than once to give consistent relative potencies, thus validating assay-to-assay reproducibility. An example of results derived from a typical antagonist assay is shown in Figure 2. As can be seen in that assay, 1 nM CRF released 4.65 ± 0.21 pg of ACTH/mL, while 0.93 ± 0.08 pg of ACTH/mL was measured in the background controls. Graded doses of the antagonist resulted in inhibition of ACTH release in a dose-related manner. From these data, relative potencies were calculated. At a time when it is common to see reports of peptidomimetics derived from combinatorial exercises that are active at micromolar if not millimolar concentrations, it is noteworthy that peptides will, in most cases, show activity in in vitro functional assays at picomolar concentrations and in vivo using micrograms/kilograms compared to milligrams/kilograms for peptidomimetics. CP-154,526, for example, antagonizes CRF-stimulated ACTH elevation in rat plasma at a concentration (mg/kg) which is at least 10 times that of α-helical $CRF_{(9-41)}$[29] which is now known to be 100 times less potent than astressin at CRFR1.[16]

Development of the potent, structurally constrained CRF antagonists and agonists presented in Table 1 resulted from the simultaneous employment of two design strategies: the D-amino acid scan (often postulated to help identify turns) and the $i-(i+3)$ lactam bridge scan that led to the discovery of astressin, a potent CRF antagonist at CRFR1 that is postulated to assume an α-helical structure.[16] To test the hypothesis that the favorable Glu[20]−Lys[23] and Glu[30]−Lys[33] lactam rings were favoring an α-helical conformation rather than a turn, we introduced a D-amino acid at positions 22, 31, and 32 of the respective rings.

We had shown that cyclo(20−23)[DPhe[12],Glu[20],Lys[23],-

124), IA 1; 19.3 (9.7−38.3), IA 25]. Agonist potencies are relative to that of ovine $CRF^{(o)}$ and/or human $CRF^{(h)}$ in the in vitro rat pituitary cell culture assay, with 95% confidence limits in parentheses. Relative potencies of oCRF and hCRF in that assay are identical. [e] The percent intrinsic activity (IA) of each of the antagonists is calculated by determining the level of secretion caused by the highest dose of antagonist (in the absence of oCRF) minus basal secretion, dividing that number by the level of secretion of 1 nM oCRF minus basal secretion, and multiplying the result by 100. [f] These particular compounds were tested two or three times.

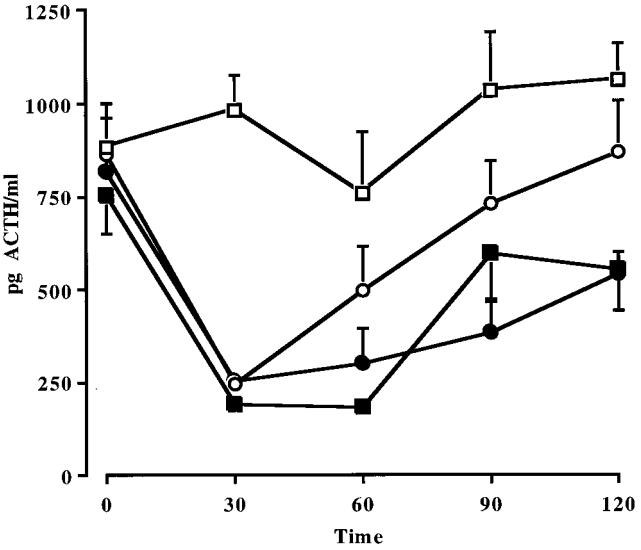

Figure 3. Effect of CRF antagonists (25 μg/adx rat, iv) on ACTH secretion. Each point represents the mean ± SEM of 3−7 animals. Data were analyzed by ANOVA followed by Duncan's multiple range test for individual differences: vehicle, □; **3**, ■; **6**, ○; **7**, ●. Each bar represents the mean ± SEM of 3−5 animals.

Nle^{21,38}]hCRF$_{(12-41)}$ (**1**) and cyclo(30−33)[DPhe^{12},Nle^{21},-Glu^{30},Lys^{33},Nle^{38}]hCRF$_{(12-41)}$ (**3**) were approximately 3 and 32 times more potent than [DPhe^{12},Nle^{21,38}]-hCRF$_{(12-41)}$, respectively.[15,16] The corresponding linear analogues **2** and **4** were considerably less potent which was interpreted in terms of structure stabilization by the lactam bridge. The structures of these four compounds (particularly that of **3**, the most potent antagonist reported to date) were the basis for further modifications. We sought to establish that these favorable cycles were indeed promoting the α-helicity documented by CD spectroscopy, rather than promoting the formation of a yet unidentified turn. On the basis of literature evidence that D-residues, by themselves[30] or within a cycle,[31] could have a dramatic effect on the potency of biologically active peptides, we introduced a D-residue within the cycle of astressin and found **5** (with DAla^{31}) to be one-half as potent and **6** (with DHis^{32}) to be twice as potent as astressin in vitro. We are aware of the fact that the relative potencies of **5** and **6**, for example, and of several other analogues described below are not statistically different (95% confidence limits overlap). Data derived from a large number of closely related analogues, however, suggest that our appreciation of the SAR is precise enough to allow the development of a successful strategy (see below in the discussion of agonists).

Since peptides are sensitive to enzyme degradation and particularly to amino- and diaminopeptidases, we also acetylated the N-terminus of **6** in an effort to increase biostability and duration of action. Potent antagonists **3**, **6**, and **7** were assayed in the adrenalectomized rat preparation described earlier,[16,32] with results presented in Figure 3. Neither the introduction of a D-residue at position 32 nor acetylation of the N-terminus had a significant effect on duration of action. These three analogues, however, are clearly more potent than the earlier generations of CRF antagonists described prior to the discovery of astressin.[16]

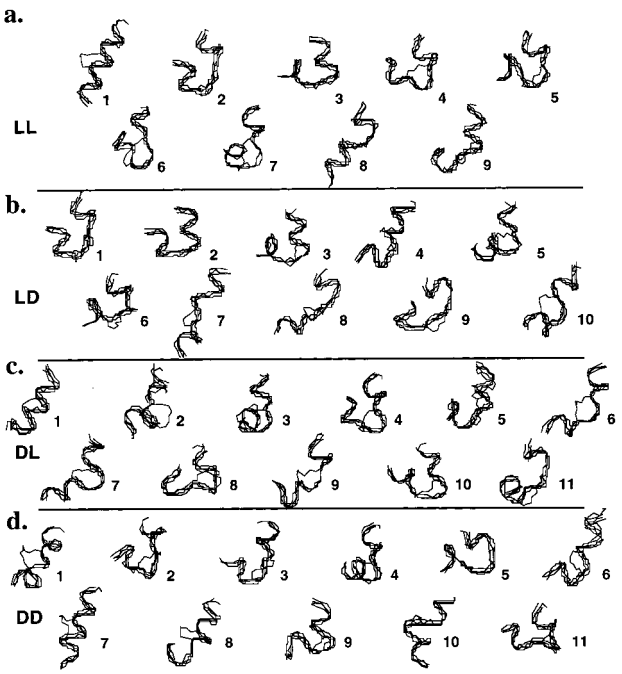

Figure 4. Ribbon diagrams of family representatives of [Glu^{5},L/DAla^{6,7},Lys^{8}]Ac-Ala$_{13}$-NH$_2$ with energies of 10.0 kcal/mol above the lowest-observed energy structure: (a) LL, [Glu^{5},-Lys^{8}]Ac-Ala$_{13}$-NH$_2$; (b) LD, [Glu^{5},DAla^{7},Lys^{8}]Ac-Ala$_{13}$-NH$_2$; (c) DL, [Glu^{5},DAla^{6},Lys^{8}]Ac-Ala$_{13}$-NH$_2$; (d) DD, [Glu^{5},DAla^{6,7},Lys^{8}]-Ac-Ala$_{13}$-NH$_2$.

Because of the high potency of **5** and **6**, we studied the structural influences of the L- to D-amino acid substitution at position (i+2) within the i−(i+3) lactam bridge on both the local and more extended regions of the molecule. In the absence of high-resolution NMR and/or X-ray crystallographic structures of **3**, molecular modeling on an Ac-Ala$_{13}$-NH$_2$ scaffold was conducted in order to quantify the structural influence of specific L- to D-amino acid (D/LXaa) substitutions. Specifically, [Glu^{5},Lys^{8}]Ac-Ala$_{13}$-NH$_2$ in a standard α-helical configuration was subjected to high-temperature molecular dynamics followed by annealing dynamics and minimization for a total cycle time of 10 ps and a total sampling time of 1 ns. A gentle restraint (5 kcal/mol/Å^2 centered about a distance of 2.1 Å) was applied to the 0−4, 1−5, and 8−12 O−H hydrogen bond donor−acceptor pairs to maintain α-helical features at the N- and C-termini. The hypothesis underlying this computational work is that the structure(s) of the potent diastereomers, astressin and **6**, stabilized by the 30−33 lactam bridge share a common conformational feature independently of the chirality of residue 32. Consequently, in parallel with the conformational search conducted on [Glu^{5},Lys^{8}]Ac-Ala$_{13}$-NH$_2$, a search was similarly conducted on the other three diastereomeric pairs of residues 6 and 7. One hundred structures for each model compound were collected. The resulting minimized structures were subjected to a family clustering algorithm which grouped all structures with rms deviations over the heavy atoms of the backbone of 2.75 Å and chose as the family representative the structure with the lowest energy within each group. For [Glu^{5},Lys^{8}]Ac-Ala$_{13}$-NH$_2$, 20 families were observed, of which the 9 representatives with energy of 10.0 kcal/mol above the lowest-energy structure (structure 1) are shown in Figure 4a. For [Glu^{5},DAla^{7},Lys^{8}]Ac-Ala$_{13}$-NH$_2$, the family clustering

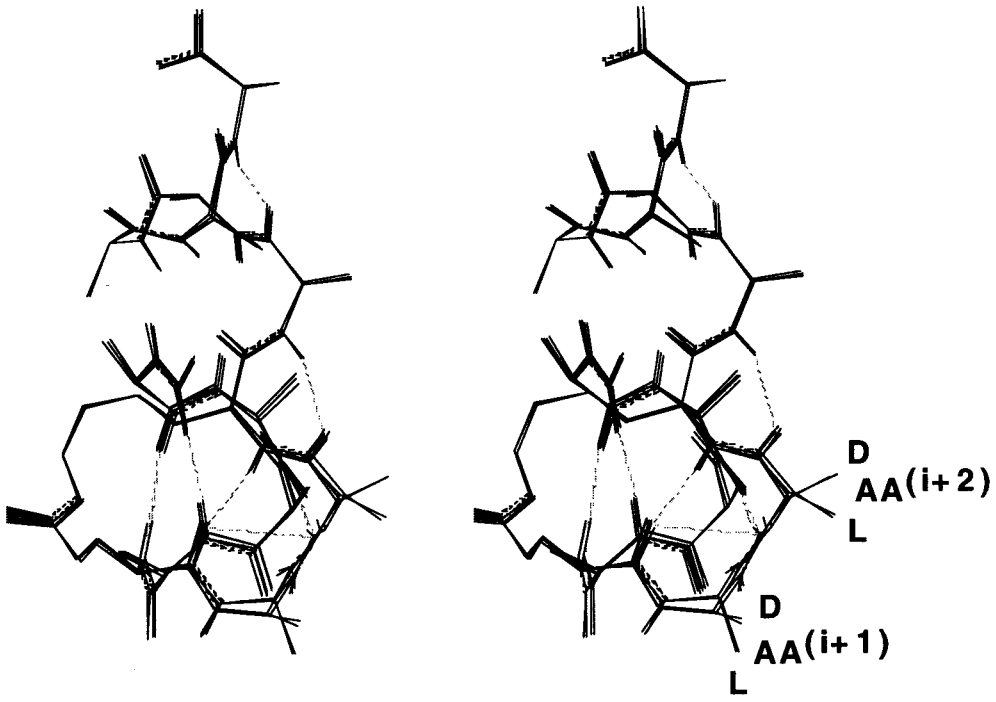

Figure 5. Stereo rendering of four diastereomers of [Glu^5,L/DAla^{6,7},Lys^8]Ac-Ala$_{13}$-NH$_2$ superposed showing heavy atoms and hydrogen bonds involving the backbone amide proton.

and energy criteria resulted in 10 representatives out of a total of 19 families identified. For both [Glu^5,DAla^6,-Lys^8]Ac-Ala$_{13}$-NH$_2$ and [Glu^5,DAla^{6,7},Lys^8]Ac-Ala$_{13}$-NH$_2$, 11 structures with energies less than 10.0 kcal/mol above the minimum found for all structures were identified out of totals of 26 structures recovered for each model. The 41 resulting structures are shown in Figure 4a−d. The backbone dihedral angles of these models are available as Supporting Information. In general, the N- and C-termini of all family representatives maintained approximately helical secondary structure due in large part to the gentle bias during the conformational search to restrain the ends of the molecules. Interestingly, fully helical structures were recovered in all diastereomers with the exception of [Glu^5,DAla^7,Lys^8]Ac-Ala$_{13}$-NH$_2$; the lowest-energy structure overall is structure 1 of the parent [Glu^5,Lys^8]Ac-Ala$_{13}$-NH$_2$, which is fully helical. Note that because the internal energy of the CVFF force field does not explicitly change upon chiral inversion of any center, the energies of the four diastereomers shown in Figure 4 are directly comparable.

Attention was then focused on the similarity between family representatives 1−9 of [Glu^5,Lys^8]Ac-Ala$_{13}$-NH$_2$ and families 1−10 of [Glu^5,DAla^7,Lys^8]Ac-Ala$_{13}$-NH$_2$ in order to look for structures where position (i+2) in the i−(i+3) lactam bridge could admit a DXaa. Within the rms deviation matrix (backbone) comparing these families, the average rms was 3.76 Å with a standard deviation of 0.85 Å and a range of 0.37−5.37 Å. Consequently, a single rms datum (0.37 Å) characterizing the superposition of family 2 of [Glu^5,Lys^8]Ac-Ala$_{13}$-NH$_2$ with family 1 of [Glu^5,DAla^7,Lys^8]Ac-Ala$_{13}$-NH$_2$ lies almost 3.9σ below the average rms deviation and clearly stands out as a single compelling example of structural similarity despite chiral difference at position 7. In fact, similar turn structures were subsequently found to have occurred spontaneously during the high-temperature conformational search and annealing of all four diastereomeric models (see Figure 4). The reason for this apparent conformational ubiquity is shown in Figure 5, which is a stereo-superposition of the four diastereomeric models template-forced to the common turn−helix−turn motif. The side chains of residues 6−7 in the Ac-Ala$_{13}$-NH$_2$ host corresponding to residues 31−32 of CRF face away from the bulk of the molecule such that the steric contribution of either diastereomer is approximately equal. In the lowest-energy structure found to date, the four diastereomers can achieve an rms deviation over the backbone atoms of Ac-Ala$_{13}$-NH$_2$ of 0.2 Å with less than 10.0 kcal/mol strain energy. Using the lower-energy member of this pair (family 2 of [Glu^5,Lys^8]Ac-Ala$_{13}$-NH$_2$) as a structural template, the residues were mutated to those of the corresponding residues 26−38 of hCRF in order to determine if any obvious structural pathology would attend CRF assuming this model conformation. After the side chains of the hCRF$_{(26-38)}$ fragment were allowed to relieve the steric strain of construction via backbone-tethered minimization, the resulting trisdecamer appears to be well-built with interesting stabilizing features that arise naturally. In this model, if the N- and C-termini of hCRF assume helical conformations, they could form a helix−turn−helix motif with Gln^{26} in close enough proximity to Lys^{36} to suggest that a lactam or other bridge could be introduced between them. This hypothesis was tested with the synthesis of **8** with a cystine bridge between residues 26 and 36. Interestingly, this peptide is active suggesting that either the cystine bridge or the folded structure induced by that constraint is not incompatible with receptor binding. The suggestion that this structural model might represent the active conformation of hCRF awaits more detailed analogue and physical biochemical studies.

The cumulative effect of the introduction of two D-residues at positions 31 and 32 resulted in **9** with

lower than expected potency (7% that of **6**) arguing for a distortion of the ring structure (with respect to that of the bioactive one) brought about by simultaneous inversion of chirality at both positions. On the other hand, the cumulative effect of the introduction of the two favored cycles [residues 20−23 and 30−33 with (**11**) or without (**10**) a D-residue at positions 22 and 32] yielded analogues approximately 5 times less potent than **6** suggesting a mild distortion of the bioactive conformation brought about by the combination of these two cycles.

At this point we wanted to confirm that the observations made with analogues of hCRF could be paralleled with analogues of the members of the CRF family known to be somewhat selective for the CRFR2. In all cases studied (the urotensin analogue **12**, the urocortin analogue **15**, and more particularly the sauvagine analogues **13** and **14**), antagonist potencies of CRF-stimulated ACTH secretion mediated by CRFR1 were significantly less than expected (20−500% that of [DPhe^{12},Nle^{21,38}]hCRF$_{(12-41)}$ versus 3000% for astressin). The effect of these substitutions on the potency or affinity of these analogues to CRFR2 is still to be determined. On the basis of the hypothesis that the cycle at positions 29−32 of Ucn increased overall structural stability of the antagonists, we introduced L- and DPro at position 11 of the cyclic Ucn analogues as potential helix inducers as had been reported earlier.[33] We surmised that, if it were the case, it would confer the analogues increased potency notwithstanding that the introduction of DPro^{11} could also stabilize the analogue against aminopeptidase activity. That the relative potencies of the three analogues **15**−**17** are statistically not different from one another suggests that any of the putative structural or enzymatic arguments have only marginal weight.

While we have shown that the introduction of the D-isomer of the amino acid at position 32 of astressin had a favorable effect on potency, we wondered whether other residues such as D2Nal^{32} (**18**), DGlu^{32} (**19**), and DArg^{32} (**20**) in astressin would also be compatible. Whereas **20** is as potent as astressin, **18** and **19** were approximately 5 times less potent. This effect is comparatively small in view of the fact that 2Nal and Glu are bulky hydrophobic on one hand and acidic on the other as compared to His. This suggests great tolerance with respect to the nature of residue 32; indeed His, Glu, Ala, and Gly are found in that position in hCRF, hUcn, Sau, and sUtn, respectively. This observation is in accord with the helix−turn−helix model (Figure 5) in that substitutions at position 31 or 32 should not necessarily perturb the overall bioactive fold.

In parallel with these studies, we investigated the effect of similar modifications on the potency of CRF agonists. First, we found that the introduction of a 20−23 cycle in a shortened CRF analogue with known favorable deletions (residues 1−3), acetylation of the N-terminus, and DPhe^{12} and Nle^{21,38} substitutions such as in **21** were compatible with high potency in the agonist series. Similarly, the additional substitution of Ala^{22} by DAla^{22} in **21** yielded **22** which was one-half as potent as **21** and the corresponding linear analogue **23**. These results (although it should be reemphasized that the relative potencies of most of the agonists described here are not different from each other) are consistent with results presented earlier for analogues having a similar *i*, (*i*+3) cycle at positions 30 and 33 (cyclic **24** and linear **25**)[16] and confirmed with the introduction of a DHis at position 32 (**26**). Similarly, substituting DAla^{31} for Ala^{31} (**27**) or DAla^{22} and DHis^{32} (**28**) for Ala^{22} and His^{32} resulted in a 2−5-fold loss of potency, paralleling results found in the antagonist series.

In fact, the effect of the introduction of a D-residue at position 32 in α-hel-CRF$_{(4-41)}$ (**29**−**31**) and carp urotensin (**32**−**34**) or equivalent [position 31 in urocortin (**35**−**37**)] on potency and CD spectra was also investigated. Parallel and consistent results with those obtained with CRF were obtained suggesting that the lactam cyclization at residues 20−23 and 30−33 (29−32 for the members of the CRF family with 40 amino acids) and a D-residue at positions 22 (21, respectively) and 32 (31, respectively) will have parallel effects. Within this series, it was surprising to find that the linear analogue **40** of sauvagine was significantly less potent than the corresponding cyclic analogue (**39**), yet this result is consistent with biological results obtained with the corresponding agonist without the DXaa^{32} substitution.[1] These results suggest that the C-terminal residues (9−41) of the CRF molecule are mostly responsible for binding and that increased binding brought about by any substitution in that fragment will have a positive effect on the potency of both agonists and antagonists.

In conclusion, we have investigated the biological consequences of subtle modification of two general classes of *i*−(*i*+3) lactam bridge in CRF and members of the CRF family by modification of the chirality of intrabridge residues. In the course of a theoretical treatment of the available conformations of a bridged trisdecaalanyl parent, a model featuring a helix−turn−helix motif with the turn centered about residues 31−32 arose spontaneously from the calculations and has been found consistent with previous SAR and biophysical studies of CRF. In this model, CRF or an antagonist assumes a predominantly helical bioactive structure with a reversal of the helical axis commencing about residue 30. Chiral inversion of residue 31 or 32 results in no statistically significant change in potency; however, chiral inversion of residues 31 and 32 results in significant loss of potency. DHis^{32} substitution in astressin (**3**) combined with acetylation of the N-terminus yields the very potent **7**, the potency of which, however, is not statistically different from that of **6**. Parallel substitutions [*i*, (*i*+3) cyclization and introduction of a D-residue at (*i*+2)] in antagonist members of the CRF family known to be CRFR2-selective (urotensin, sauvagine, and urocortin) do not result in a parallel improvement of potency at CRFR1 suggesting that these modifications may induce additional selectivity, a hypothesis yet to be tested. In the agonist series, the same modifications have a much lesser impact on biological potency suggesting again that the stabilizing effect of the lactam ring in the antagonist series may be inducing a structural constraint brought about otherwise by the N-terminal residues responsible for agonism.

Experimental Section

Synthesis of CRF Analogues. All analogues shown in Table 1 were synthesized either manually or on a Beckman

990 peptide synthesizer using the solid-phase approach, the MBHAR,[15] and the Boc strategy with orthogonal protection (Fmoc and OFm) of the side chains of residues to be cyclized.[21] Amino acid derivatives Boc-Ala, Boc-Arg(Tos), Boc-Asn(Xan), Boc-Asp(cHex), Boc-Gln(Xan), Boc-Glu(cHex), Boc-His(Tos), Boc-Ile, Boc-Met, Boc-Leu, Boc-Phe, Boc-Pro, Boc-Ser(Bzl), Boc-Thr(Bzl), Boc-Tyr(2-Br-Cbz), and Boc-Val were obtained from Bachem Inc. (Torrance, CA), Chem-Impex International (Wood Dale, IL), and Calbiochem (San Diego, CA). Boc-Glu(OFm) and Boc-Lys(Fmoc) were synthesized as described earlier.[34] All solvents were reagent grade or better. TFA, 50−60% in DCM (1% *m*-cresol), was used to remove the Boc group. Main-chain assembly was mediated by DIC. Three-fold excess protected amino acid was used based on the original substitution of the MBHAR. When the synthesis was carried out on a synthesizer, coupling time was 90−120 min followed by recoupling after residue 32 (with the exception of glycine and alanine residues which were not recoupled). Automatic acetylation (excess acetic anhydride in DCM for 15 min) was carried out after addition of each amino acid. When synthesized manually, recouplings were carried out only when necessary and acetylations only when recoupling could not yield negative ninhydrin tests.[35] Deprotection of the Fmoc group was achieved using a fresh solution of 20% piperidine/DMF or NMP (2 × 10 min) followed by sequential washes with DMF, MeOH, 10% TEA/DCM, and DCM. Lactam formation was mediated using TBTU or HBTU in DMF or NMP in the presence of 3-fold excess of DIEA. Best results were obtained when the peptide chain was assembled in its entirety prior to cleavage of the Fmoc and Ofm protecting groups and cyclization as shown earlier.[15] The peptides were cleaved and deprotected in HF in the presence of anisole (5−10%, v/v). After removal of HF under reduced pressure, the resin was washed with diethyl ether in portions. The peptide was extracted from the resin using dilute AcOH or TFA and Acn (30−60%) and lyophilized. The lyophilized powder was analyzed using analytical HPLC, and the major components were collected for mass spectrometry analysis. The desired product was therefore identified and purified using RP-HPLC and three solvent systems (TEAP at pH 2.25, TEAP at pH 4.5−6.5, and 0.1% TFA, successively).[22,23] One exception to this general approach was the synthesis of **8** which required an additional oxidation step in order to form the disulfide bond between residues 26 and 36. Starting with 2.0 g of MBHA resin substitution (0.33 mequiv/g), usual deblocking (50% TFA in DCM with 3−5% *m*-cresol as scavenger) and coupling protocols (3-fold excess of each amino acid and coupling times varying from 45 to 120 min) were followed. Under these conditions only Arg[23] had to be recoupled. γ-OFm-Glu[30] and ϵ-Fmoc-Lys[33] were deblocked using 20% piperidine in NMP (2 × 50 mL, 10 min each). Bridge formation was achieved with TBTU (3 equiv in NMP) and DIEA (9 equiv in NMP) overnight. N-Terminal Boc group was removed, and the peptidoresin was washed and dried (final weight 4.72 g). Peptidoresin was cleaved in HF (50 mL) in the presence of anisole (5 mL) for 1.5 h at 0 °C. After elimination of HF under vacuum, crude peptide was washed with peroxide-free ether and extracted with 0.1% TFA in 60% Acn/water (100 mL). After analytical identification of the desired reduced **8** by mass spectrometry, the crude peptide in its reduced form was diluted with 500 mL of distilled water and purified using preparative HPLC (cartridge 5 × 30 cm, Vydac C_{18}, 15−20 μm, 300-Å pore size, gradient 24−60% Acn in 120 min, flow rate 100 mL/min, detection at 220 nm). Fractions were collected and analyzed using analytical HPLC. The desired fraction eluted between retention volumes 7.6 and 8.7 L. An aliquot of that solution (900 mL) was neutralized to pH 7.12 with ammonia. The solution was exposed to air with slow stirring in a beaker. Because oxidation progressed very slowly under these conditions (monitored by HPLC), H_2O_2 (3%, 20 mL) was added dropwise at room temperature. Completion of cyclization (2 h) was followed by the Ellman test and by RP-HPLC. The solution was acidified (pH 2.25) with TFA (1.0 mL) and diluted to 1.8 L. This solution was applied to preparative HPLC and purified using similar conditions as above for the reduced material (only difference, gradient was 30−60% Acn in 100 min). Peptide eluted after 5.2 L. Several fractions were collected, and those deemed >97% pure were pooled and lyophilized (yield 40 mg). Side fractions (>90% pure, 25 mg) were also collected. Analytical data are reported in Table 1.

Molecular Modeling. The potential energy parameters and functional forms were from CVFF force field.[36,37] Molecular dynamics and energy minimizations were performed using discover and Insight II (MSI, Inc., San Diego, CA) on a Silicon Graphics Iris Crimson workstation.

Characterization of CRF Analogues. Peptides were characterized as shown in Table 1 and below. Most analogues were greater than 95% pure with no impurity greater than 1% using independent HPLC and CZE criteria and had expected masses.

A. RP-HPLC. In addition to determining the purity of the peptides in an acidic system (see Table 1 legend), most of the analogues were also analyzed using 0.05% TEAP at pH 6.8 and a Vydac C_8 column (0.21 × 15 cm) at a flow rate of 0.2 mL/min with slightly varying gradient slopes. Percent purity was in the range of that found with CZE or with HPLC under acidic conditions.

B. Capillary Zone Electrophoresis (CZE). CZE was carried out using a Beckman P/ACE System 2000 controlled by an IBM Personal System/2 model 50Z and using a ChromJet integrator. Electrophoresis was performed in 0.1 M sodium phosphate (pH 2.5) except for α-hel-$CRF_{(9-41)}$ which was measured in 0.1 M sodium borate (pH 8.5). Acn (30%) was added to the buffers in order to gain sharp elution profiles.[38]

C. Mass Spectroscopy. LSIMS mass spectra were measured with a JEOL JMS-HX110 double focusing mass spectrometer (JEOL, Tokyo, Japan) fitted with a Cs^+ gun. An accelerating voltage of 10 kV and Cs^+ gun voltage of 25 kV were employed; for further details, see ref 15. Calculated values for protonated molecular ions were in agreement with those observed using liquid secondary ion mass spectrometry.

D. CD Spectropolarimetry. CD spectra for compounds **3**−**6**, **9**, and **11** were collected on an Aviv model 62DS spectropolarimeter (Aviv Associates, New Jersey) operated under the control of the manufacturer's 60DS software. Samples were dissolved in MilliQ water and showed no evidence of light scattering. Collection conditions: 260−185 nm, 1.0 nm/point, 1.0-s integration time, 1.5-nm bandwidth, 4 repetitions, T = 20.0 °C. The maximum photomultiplier (PM) voltage for compounds **3**−**6** and **9** was 390 V @ 185 nm; the maximum PM voltage for compound **11** was 550 V @ 185 nm. No postcollection smoothing was applied to the spectra.

E. In Vitro Pituitary Cell Culture Assay. Rat anterior pituitary glands from male Sprague−Dawley rats were dissociated by collagenase treatment and plated (0.16×10^6 cells/well in 48-well plates) in medium containing 2% fetal bovine serum (FBS).[27] Three days after plating, the cells were washed three times with fresh medium containing 0.1% bovine serum albumin (BSA) and incubated for 1 h. Following the 1-h preincubation, the cells were washed once more and the test peptides were applied in the absence (determination of intrinsic activity) or the presence (testing of antagonistic activity) of 1 nM oCRF. Controls with no treatment were also introduced at the beginning and end of the assay to account for any variability and averaged. At the end of a 3-h incubation period, the media were collected and the level of ACTH was determined by radioimmunoassay (Diagnostic Products Corp.). When not mentioned IA = 100%. Because we report relative potencies, it is important to mention that the standards used over the years were made in single large batches that are used year after year and are weighed and serially diluted by the same individuals. The stability of the batches is checked on a regular basis using HPLC and CZE. This does not exclude the possibility that once in a while results do not correlate as well as one would want. Under these circumstances the assays are repeated; yet when we see no justifiable reason to discard the "faulty" results (as the case here for **6**), we average the data (see legend to Table 1).

In Vivo Adrenalectomized Rat Assay. Adult male rats (ca. 230 g) were adrenalectomized under halothane anesthesia 8 days prior to the experiments. Their diet was supplemented with oranges, and their water contained 0.9% NaCl. They were equipped with indwelling jugular cannulae[32] 48 h prior to the iv injection of the vehicle or the antagonists (100 μg/kg in 0.5 mL). All protocols were approved by the Salk Institute IACUC. Analogues were first diluted in sterile distilled water, and the pH was adjusted to 7.0. Further dilutions were made in 0.04 M phosphate buffer, pH 7.4, containing 0.1% BSA and 0.01% ascorbic acid. Blood samples (0.3 mL) were obtained immediately before treatment as well as at 30, 60, 90, and 120 min later (Figure 2). Decanted plasma were frozen until assayed for ACTH concentrations with a commercially available kit (Allegro Kit, Nichols Institute, San Juan Capistrano, CA).[32]

Acknowledgment. This work was supported in part by NIH Grant DK-26741, The Hearst Foundation, and the Foundation for Research, California Division. Drs. W. Vale, C. Rivier, and A. G. Craig are FR Investigators. We thank C. Miller, R. Kaiser, D. Kirby, T. Goedken, and Y. Haas for technical assistance, Dr. J. Erchegyi for the synthesis of **31**, L. Cervini for critical review of the manuscript, and D. Johns for manuscript preparation.

Supporting Information Available: Backbone dihedral angles of family representative structures of [Glu^5,L/DAla^{6,7},-Lys^8]Ac-Ala$_{13}$-NH$_2$ with energies of 10.0 kcal/mol above the lowest observed energy structure (2 pages). Ordering information can be found on any current masthead page.

References

(1) Rivier, J.; Lahrichi, S. L.; Gulyas, J.; Erchegyi, J.; Koerber, S. C.; Craig, A. G.; Corrigan, A.; Rivier, C.; Vale, W. Minimal-size, constrained corticotropin releasing factor agonists with *i*-(*i*+3) Glu-Lys and Lys-Glu bridges. *J. Med. Chem.* **1998**, *41*, 2614−2620.

(2) Vale, W.; Spiess, J.; Rivier, C.; Rivier, J. Characterization of a 41 residue ovine hypothalamic peptide that stimulates the secretion of corticotropin and β-endorphin. *Science* **1981**, *213*, 1394−1397.

(3) Rivier, C. L.; Plotsky, P. M. Mediation by corticotropin-releasing factor (CRF) of adenohypophysial hormone secretion. *Annu. Rev. Physiol.* **1986**, *48*, 475−494.

(4) Chen, R.; Lewis, K. A.; Perrin, M. H.; Vale, W. W. Expression cloning of a human corticotropin releasing factor (CRF) receptor. *Proc. Natl. Acad. Sci. U.S.A.* **1993**, *90*, 8967−8971.

(5) Chang, C. P.; Pearse, R. V., II; O'Connell, S.; Rosenfeld, M. G. Identification of a seven transmembrane helix receptor for corticotropin-releasing factor and sauvagine in mammalian brain. *Neuron* **1993**, *11*, 1187−1195.

(6) Perrin, M.; Donaldson, C.; Chen, R.; Blount, A.; Berggren, T.; Bilezikjian, L.; Sawchenko, P.; Vale, W. Identification of a second CRF receptor gene and characterization of a cDNA expressed in heart. *Proc. Natl. Acad. Sci. U.S.A.* **1995**, *92*, 2969−2973.

(7) Kishimoto, T.; Pearse, R. V., II; Lin, C. R.; Rosenfeld, M. G. A sauvagine/corticotropin-releasing factor receptor expressed in heart and skeletal muscle. *Proc. Natl. Acad. Sci. U.S.A.* **1995**, *92*, 1108−1112.

(8) Vita, N.; Laurent, P.; Lefort, S.; Chalon, P.; Lelias, J. M.; Kaghad, M.; Le, F. G.; Caput, D.; Ferrara, P. Primary structure and functional expression of mouse pituitary and human brain corticotropin releasing factor receptors. *FEBS Lett.* **1993**, *335*, 1−5.

(9) Lovenberg, T. W.; Liaw, C. W.; Grigoriadis, D. E.; Clevenger, W.; Chalmers, D. T.; DeSouza, E. B.; Oltersdorf, T. Cloning and characterization of a functionally distinct corticotropin-releasing factor receptor subtype from rat brain. *Proc. Natl. Acad. Sci. U.S.A.* **1995**, *92*, 836−840.

(10) Perrin, M. H.; Donaldson, C. J.; Chen, R.; Lewis, K. A.; Vale, W. W. Cloning and functional expression of a rat brain corticotropin releasing factor (CRF) receptor. *Endocrinology* **1993**, *133*, 3058−3061.

(11) *Corticotropin-Releasing Factor*; Vale, W., Eds.; John Wiley & Sons: West Sussex, England, 1993; Ciba Foundation Symposium 172, p 357.

(12) Munck, A.; Guyre, P. M. Glucocorticoid physiology, pharmacology and stress. *Adv. Exp. Med. Biol.* **1986**, *196*, 81−96.

(13) Dallman, M. F.; Strack, A. M.; Akana, S. F.; Bradbury, M. J.; Hanson, E. S.; Scribner, K. A.; Smith, M. Feast and famine: critical role of glucocorticoids with insulin in daily energy flow. *Front. Neuroendocrinol.* **1993**, *14*, 303−347.

(14) Hernandez, J.-F.; Kornreich, W.; Rivier, C.; Miranda, A.; Yamamoto, G.; Andrews, J.; Taché, Y.; Vale, W.; Rivier, J. Synthesis and relative potencies of new constrained CRF antagonists. *J. Med. Chem.* **1993**, *36*, 2860−2867.

(15) Miranda, A.; Koerber, S. C.; Gulyas, J.; Lahrichi, S.; Craig, A. G.; Corrigan, A.; Hagler, A.; Rivier, C.; Vale, W.; Rivier, J. Conformationally restricted competitive antagonists of human/rat corticotropin-releasing factor. *J. Med. Chem.* **1994**, *37*, 1450−1459.

(16) Gulyas, J.; Rivier, C.; Perrin, M.; Koerber, S. C.; Sutton, S.; Corrigan, A.; Lahrichi, S. L.; Craig, A. G.; Vale, W.; Rivier, J. Potent, structurally constrained agonists and competitive antagonists of corticotropin releasing factor (CRF). *Proc. Natl. Acad. Sci. U.S.A.* **1995**, *92*, 10575−10579.

(17) Miranda, A.; Lahrichi, S. L.; Gulyas, J.; Koerber, S. C.; Craig, A. G.; Corrigan, A.; Rivier, C.; Vale, W.; Rivier, J. Constrained corticotropin releasing factor (CRF) antagonists with i-(i+3) Glu- - -Lys bridges. *J. Med. Chem.* **1997**, *40*, 3651−3658.

(18) Pallai, P. V.; Mabilia, M.; Goodman, M.; Vale, W.; Rivier, J. Structural homology of corticotropin-releasing factor, sauvagine, and urotensin I: Circular dichroism and prediction studies. *Proc. Natl. Acad. Sci. U.S.A.* **1983**, *80*, 6770−6774.

(19) Romier, C.; Bernassau, J.-M.; Cambillau, C.; Darbon, H. Solution structure of human corticotropin releasing factor by ^{1}H NMR and distance geometry with restrained molecular dynamics. *Protein Eng.* **1993**, *6*, 149−156.

(20) Rivier, J.; Rivier, C.; Galyean, R.; Miranda, A.; Miller, C.; Craig, A. G.; Yamamoto, G.; Brown, M.; Vale, W. Single point D-substituted corticotropin releasing factor analogues: Effects on potency and physicochemical characteristics. *J. Med. Chem.* **1993**, *36*, 2851−2859.

(21) Felix, A. M.; Heimer, E. P.; Wang, C. T.; Lambros, T. J.; Fournier, A.; Mowles, T. F.; Maines, S.; Campbell, R. M.; Wegrzynski, B. B.; Toome, V.; Fry, D.; Madison, V. S. Synthesis, biological activity and conformational analysis of cyclic GRF analogues. *Int. J. Pept. Protein Res.* **1988**, *32*, 441−454.

(22) Hoeger, C.; Galyean, R.; Boublik, J.; McClintock, R.; Rivier, J. Preparative reversed phase high performance liquid chromatography. II. Effects of buffer pH on the purification of synthetic peptides. *Biochromatography* **1987**, *2*, 134−142.

(23) Rivier, J. Use of trialkylammonium phosphate (TAAP) buffers in reverse phase HPLC for high resolution and high recovery of peptides and proteins. *J. Liq. Chromatogr.* **1978**, *1*, 343−367.

(24) Yang, J. T.; Wu, C.-S. C.; Martinez, H. M. Calculation of protein conformation from circular dichroism. In *Methods in Enzymology;* Hirs, C. H. W., Timasheff, S. N., Eds.; Academic Press: New York, 1986; Vol. 130, p 228.

(25) Böhm, G.; Muhr, R.; Jaenicke, R. Quantitative analysis of protein far UV circular dichroism spectra by neural networks. *Protein Eng.* **1992**, *5*, 191−195.

(26) Rivier, J.; Rivier, C.; Vale, W. Synthetic competitive antagonists of corticotropin releasing factor: Effect on ACTH secretion in the rat. *Science* **1984**, *224*, 889−891.

(27) Vale, W.; Vaughan, J.; Yamamoto, G.; Bruhn, T.; Douglas, C.; Dalton, D.; Rivier, C.; Rivier, J. Assay of corticotropin releasing factor. In *Methods in Enzymology: Neuroendocrine Peptides;* Conn, P. M., Ed.; Academic Press: New York, 1983; Vol. 103, pp 565−577.

(28) Rivier, J.; Spiess, J.; Vale, W. Characterization of rat hypothalamic corticotropin-releasing factor. *Proc. Natl. Acad. Sci. U.S.A.* **1983**, *80*, 4851−4855.

(29) Schulz, D. W.; Mansbach, R. S.; Sprouse, J.; Braselton, J. P.; Collins, J.; Corman, M.; Dunaiskis, A.; Faraci, S.; Schmidt, A. W.; Seeger, T.; Seymour, P.; Tingley, F. D., III; Winston, E. N.; Chen, Y. L.; Heym, J. CP-154,526: A potent and selective nonpeptide antagonist of corticotropin releasing factor receptors. *Proc. Natl. Acad. Sci. U.S.A.* **1996**, *93*, 10477−10482.

(30) Monahan, M.; Amoss, M.; Anderson, H.; Vale, W. Synthetic analogues of the hypothalamic luteinizing hormone releasing factor with increased agonist or antagonist properties. *Biochemistry* **1973**, *12*, 4616−4620.

(31) Rivier, J.; Brown, M.; Vale, W. [D-Trp^8]-somatostatin: An analogue of somatostatin more potent than the native molecule. *Biochem. Biophys. Res. Commun.* **1975**, *65*, 746−751.

(32) Rivier, C.; Shen, G. H. In the rat, endogenous nitric oxide modulates the response of the hypothalamic-pituitary-adrenal axis to interleukin-1β, vasopressin and oxytocin. *J. Neurosci.* **1994**, *14*, 1985−1993.

(33) Chou, P. Y.; Fasman, G. D. Empirical predictions of protein conformation. *Annu. Rev. Biochem.* **1978**, *47*, 251−276.

(34) Felix, A. M.; Wang, C.-T.; Heimer, E. P.; Fournier, A. Applications of BOP reagent in solid-phase synthesis. II. Solid-phase side-chain to side-chain cyclizations using BOP reagent. *Int. J. Pept. Protein Res.* **1988**, *31*, 231−238.
(35) Kaiser, E.; Colescott, R. L.; Bossinger, C. D.; Cook, P. I. Color test for detection of free terminal amino groups in the solid-phase synthesis of peptides. *Anal. Biochem.* **1970**, *34*, 595−598.
(36) Maple, J.; Dinur, U.; Hagler, A. T. Derivation of force fields for molecular mechanics and dynamics from Ab Initio energy surfaces. *Proc. Natl. Acad. Sci. U.S.A.* **1988**, *85*, 5350−5354.
(37) Maple, J. R.; Thacher, T. S.; Dinur, U.; Hagler, A. T. Biosym force field research results in new techniques for the extraction of inter- and intramolecular forces. *Chem. Design Automation News* **1990**, *5*, 5−10.
(38) Miller, C.; Rivier, J. Analysis of synthetic peptides by capillary zone electrophoresis in organic/aqueous buffers. *J. Pept. Res.* **1998**, *51*, 444−451.

JM980350K